



Diseño de una estrategia de control para la gestión óptima de un sistema híbrido de energía basado en paneles solares y sistema de almacenamiento

Basantes Panchi, Jonathan Andres y Paredes Troya, Daniela Estefanía

Departamento de Eléctrica y Electrónica

Carrera de Ingeniería en Electrónica e Instrumentación

Artículo académico, previo a la obtención del título de Ingeniero en Electrónica e Instrumentación

Directora: Ing. Llanos Proaño, Jacqueline del Rosario Ph.D

Co - Director: Ortiz Villalba, Diego Edmundo Ph.D

3 de marzo del 2023

Energy Management System (EMS) Based on Model Predictive Control (MPC) for an Isolated DC Microgrid

Jonathan Andrés Basantes ^{1,*}, Daniela Estefanía Paredes ^{1,*}, Jacqueline Rosario Llanos ^{1,*}, Diego Ortiz Villalba¹ and Claudio Burgos ²

¹ Department of Electrical and Electronic Engineering, Universidad de las Fuerzas Armadas (ESPE), Sangolquí 171103, Ecuador

² Institute of Engineering Sciences, Universidad de O'Higgins, Rancagua 2820000, Chile

* Correspondence: jabasantes1@espe.edu.ec (J.A.B); danieparedes4@gmail.com (D.E.P); jdllanos1@espe.edu.ec (J.L.P)

Abstract: Microgrids have become an alternative for integrating distributed generation to supply energy to isolated communities, so their control and optimal management are important. This research designs and simulates the three levels of control of a DC microgrid operating in isolated mode, proposes an Energy Management System (EMS) based on Model Predictive Control (MPC), with real-time measurement feedback for optimal energy dispatch, which ensures power flow distribution and operation at minimum cost while extending the lifespan of the BESS. The EMS can react to disturbances produced in the lower control levels. The microgrid's performance is analyzed and compared in two scenarios without EMS, and with EMS against changes in irradiation and changes in electricity demand. The fulfillment of the power balance is evaluated by analyzing the power delivered by each generation unit, the operating cost, and the state of charge of the battery (SOC).

Keywords: droop control; energy management system; microgrid; battery energy storage system; voltage restorer; state of charge.

1. Introduction

Currently, energy production is based on the consumption of fossil resources, which is an expensive process that leads to the depletion of available non-renewable resources. Therefore, the importance of the use of natural resources (renewable resources) arises at the time of introducing other forms of sustainable electricity production, supporting the environment, since this resource does not generate pollution [1,2].

The energy needs facing the world and the increase in energy consumption in the coming years make it necessary to increase the generation of electric power, which is restricted by the reduction of fossil fuel reserves and the harmful impact it has on the environment [3]. Therefore, it is important to know the term microgrids, composed of energy generation sources such as solar, wind, biomass, geothermal, hydroelectric, and fossil, among others. In addition to integrating storage systems to supply local loads [4].

The classification of microgrids is very broad because they can operate in AC current, DC current, or both. Microgrids can operate in isolated mode and grid-connected mode, allowing disconnection and connection to the conventional distribution network. Isolated microgrids arise from the need to supply energy to sectors of difficult access, whether isolated or rural areas, which for the most part do not have access to electric power service [3,5,6].

Traditionally, microgrids have a three-tier hierarchical control architecture. The primary control includes the local controllers to regulate frequency and voltage and the Droop Control for power sharing in the dispatchable generation units. The secondary control is in charge of restoring frequency and voltage [7]. Finally, the tertiary control is in charge of the optimal management of the microgrid [8,9,10].

Citation: To be added by editorial staff during production.

Academic Editor: Firstname Last-name

Received: date
Accepted: date
Published: date

Publisher's Note: MDPI stays neutral with regard to jurisdictional claims in published maps and institutional affiliations.



Copyright: © 2022 by the authors. Submitted for possible open access publication under the terms and conditions of the Creative Commons Attribution (CC BY) license (<https://creativecommons.org/licenses/by/4.0/>).

Therefore, microgrids have gained attention as a new alternative to face the energy transition and the challenges of energy supply, due to their versatility to operate in isolated or grid-connected mode [8]. Among the main contributions of microgrids in the energy market, it stands out that they are more efficient, reduces CO₂ emissions, encourages the use of renewable energies, and reduces energy costs. In addition to the above, microgrids are not centrally planned or managed [4,5].

Currently, the distribution of DC energy through microgrids is a topic of research interest for residential applications, due to the increase in DC loads, the implementation of energy sources based on renewable resources, and the development of power electronics and storage systems [11,12].

The advantages of DC microgrids are reduction of power losses, increases system efficiency, integration of distributed generation technologies through control and monitoring, and cost reduction. They also can supply energy to a load independently when voltage fluctuations occur, ensuring an efficient, reliable, and safe system [11,13,14].

It is important to note that failure to properly manage a microgrid leads to a waste of energy resources, making it an inefficient operation. Therefore, an adequate management system is necessary to manage the energy flow of the generation units, this can be achieved with intelligent and optimal control strategies, that is how the term energy management system (EMS) appears.

EMS is important in controlling the generation and distribution of power flow in microgrids and, therefore, minimizing operating costs [14,15]. Therefore, a control system based on MPC (Model Predictive Control) optimization is proposed, which makes explicit use of the mathematical model of the process, in addition to considering the objective function that seeks to minimize the operating cost of the system [16,17,18].

There are some EMS proposals for DC microgrids, which apply various control methods. In [19], an isolated microgrid consisting of two renewable sources, a diesel generator, and a storage system is developed. The objective is to maximize the useful life of the batteries and minimize the cost of energy generation, using the multiobjective genetic algorithm NSGA-II. As a result of the optimization algorithm, several solutions are obtained which meet the cost-minimization requirements. Therefore, it is up to the researchers to select the solution that fits the physical conditions of the microgrid.

In the same context of EMS applied to DC microgrids, [44] presents a predictive control of a microgrid that can operate in island mode or grid-connected mode, using a distributed control architecture, i.e., integrating a MPC for each generation unit (wind generator and photovoltaic generator) and another MPC for the energy storage unit, therefore, this type of control makes decisions individually. In addition, management based on heuristic methods is evidenced, ensuring that the management system determines the operation mode of the microgrid based on the generated power, demand, solar irradiance, wind speed, the nominal power of the units, and the SOC of the BESS.

Meanwhile, in [20] and [21], the MPC control strategy is implemented to optimally manage the load sharing between generation sources, storage, and interaction with the grid if necessary. However, the management system solves the optimization problem without real-time feedback on the actual battery states.

The authors in [22] and [23] propose an energy management system (EMS), [22] based on a MOGA algorithm (multi-objective genetic algorithm) with a 51% reduction in operational costs and a 96% reduction in the amount of pollutant gas emissions. In [23] addition to an EMS, they implement a demand-side management (DSM) that consists of modifying the consumption within a certain range of time, to reduce the cost and adjust the generation profiles of energy.

In [24] they use an advanced control for the management of a DC microgrid that operates in island mode through a MPC model integrating artificial intelligence (AI), where AI replaces mathematical modeling, typically used when working with complex and accurate mathematical models. Demonstrating that the controller is capable to provide

47
48
49
50
51
52
53
54
55
56
57
58
59
60
61
62
63
64
65
66
67
68
69
70
71
72
73
74
75
76
77
78
79
80
81
82
83
84
85
86
87
88
89
90
91
92
93
94
95
96
97
98
99
100

efficient control actions for optimal energy management and a correct energy balance for the microgrid.

In [25] analyzes the optimization of isolated AC microgrids that include several renewable sources and energy storage, focusing on several systems connected in the same microgrid. Therefore, for the interconnection of the microgrids, a distributed control based on the DMPC model is developed since it considers each unit as a subsystem and will be controlled by a local MPC being fundamental to know the information to be exchanged between each unit. In addition, for integrating electric vehicles (EV), it was necessary to develop an EMS to manage the use of vehicle batteries. Furthermore, [25] and [26] realize the integration of electric vehicles (EV) therefore the development of an EMS to manage the use of vehicle batteries is necessary.

In the previously reported works, the local controllers are not designed, nor was there online feedback on the measurements that show the current state of the batteries in the EMS system. Therefore, a control strategy is considered, with no feedback from the actual measurements, i.e., it is assumed that everything works correctly. However, disturbances at that level are not identified by the EMS.

This research paper proposes the design of a tertiary EMS control for an isolated DC microgrid, consisting of a photovoltaic system that takes full advantage of the solar resource, a diesel generator as a backup power source, a battery energy storage system, and a DC load.

The photovoltaic system is connected to the Bus DC through the Boost-type DC/DC power converter, which contains an MPPT based on the incremental conductance algorithm (INC). On the other hand, the diesel generator will operate only when necessary. The storage system, consisting of a battery bank, is connected to the Bus DC through a bidirectional Buck-Boost topology converter that allows operation in charge and discharge mode of the storage system.

The control of the microgrid is performed by a local PI voltage and current controller, which allows maintaining a constant voltage on the Bus DC and the Droop Control to share the power generated by each generation unit. While the optimal management is performed by an EMS, which allows optimal and efficient decision making in the management of the system, controlling several generation units including a photovoltaic system, BESS storage system and a diesel generator, which will be able to feed a DC load.

All control levels are designed, but mainly in this work, an EMS based on MPC is proposed to maximize the consumption of energy based on renewable resources (sun) and minimizing the consumption of energy from the diesel generator and costs for your energy consumption. It also has the scope of increasing the useful life of the battery while respecting the SOC, guaranteeing optimal charging and discharging.

The main contributions of this research work are: i) Proposing a control strategy for the optimal management of an isolated DC microgrid, maximizing the use of solar resources, extending battery life, and minimizing the operating cost of the microgrid, through the optimal distribution of power, based on linear programming guaranteeing the global optimum ii) Design and simulate all levels of control, integrating primary, secondary and tertiary control, making measurements in real-time which allows understanding the operation of the microgrid in a couple, where the tertiary control (EMS) responds to changes in the lower control levels when disturbances occur, therefore the operation of the DC microgrid is integral, iii) The tertiary control is based on MPC operating in sliding mode, in this way the EMS designed allows reacting to rapid changes in demand and irradiation, being able to detect changes in input variables.

The rest of this document is organized as follows: the system description (Section 2) shows each of the elements that make up the microgrid and how it will be controlled by the EMS. The design of the control and management algorithms of a DC microgrid is presented (Section 3) where the architecture of each control level is explained in detail. The results (Section 4) show the comparison of the operation between a microgrid with and without the proposed EMS. The conclusions (Section 5) show a quantitative analysis of the

costs generated by not having a tertiary control that adequately manages the power supplied by each generation unit. And the optimal operation of the DC microgrid with all levels of control.

2. System Description

As mentioned above, this research proposes the control of an isolated DC microgrid as shown in Figure 1, consisting of a photovoltaic generation unit (G_{PV}), a diesel generation unit (G_D), and a battery energy storage system (BESS), connected to a bus DC which supplies power to a DC-type load at a constant power.

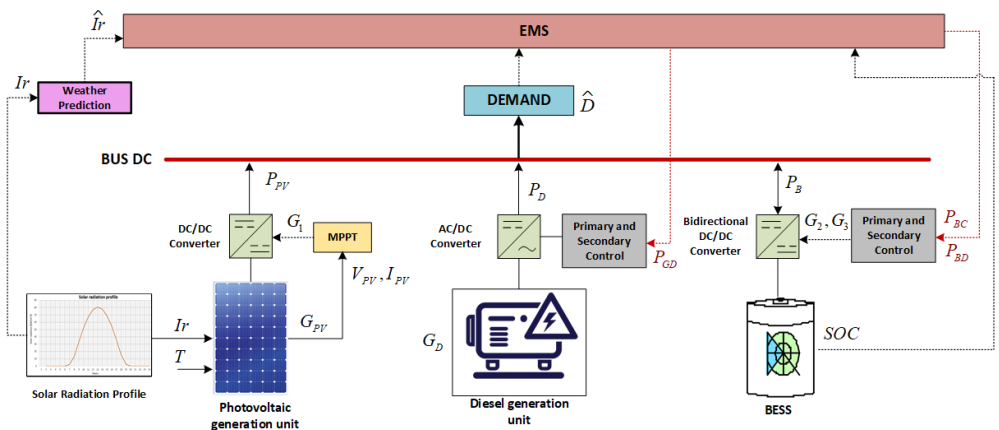


Figure 1. DC Microgrid configuration diagram.

The photovoltaic generation unit captures solar irradiation (I_r), transforming it into electricity, an energy that is injected into the Bus DC to supply demand; it is also important to note that I_r is an input to a prediction model and its output (\hat{I}_r) will be the input to the EMS optimization problem. The photovoltaic panels have a voltage response V_{PV} and current I_{PV} depending mainly on the solar irradiance (I_r), and temperature (T), which are external factors that directly affect its operation [27]. This unit provides photovoltaic power represented by (P_{PV}) which is controlled by an incremental conductance MPPT that generates the G_1 trigger to activate the IGBT of the DC/DC converter.

On the other hand, the diesel generator is in charge of transforming the fuel into electrical energy, represented as diesel power (P_D). Its main objective in microgrids is to be an auxiliary unit as a support in case the predicted electrical demand (\hat{D}) is not covered by other generation units. Its operation depends on the diesel generator power calculated by the EMS (P_{CD}). This diesel generation unit, being an alternating current source, needs an AC/DC converter to be implemented in a DC microgrid, thus performing the conversion to be able to feed the direct current load.

The battery energy storage system (BESS) will be able to deliver energy on demand, expressed as the battery power (P_B) which can operate in charge mode when (P_B) has a negative sign and discharge mode when it has a positive sign. However, in the process of charging and discharging the battery, overloads and deep discharges cannot be allowed indefinitely, since this seriously compromises their useful life. Therefore, the SOC (State of charge) is important for the analysis between the amount of power that can be obtained from the battery with respect to the total power. In order to keep the batteries within the safe operating threshold, control strategies are implemented to prolong their useful life.

These modes of operation are performed by the bidirectional DC/DC converter regulated by the EMS control signal, battery discharge power calculated by the EMS (P_{BD}) battery charge power calculated by the EMS P_{BC} , allowing generate the triggers in G_2 and G_3 for the activation of the IGBT circuit breakers on the values of P_{BC} and P_{BD} provided by the EMS.

Therefore, the different levels of control are designed and analyzed, the first level corresponds to the local control that constitutes the voltage and current controllers, the Droop Control and voltage regulators; and finally, an EMS management system. It is important to consider that the EMS is based on a MPC controller, capable of making optimal and efficient decisions in the management of the DC microgrid, based on the real-time status of variables such as the state of the battery.

3. DC Design of Control and Management Algorithms of a DC Microgrid

This section shows the control levels implemented in the DC microgrid (Figure 2). The lowest level of the control architecture is Primary control (light blue section) where the primary controllers in charge of keeping the generation levels regulated and distributing the power based on the capacity of the generation units are located. The Secondary control (orange section) represents the control in charge of restoring the voltage to its nominal value. Finally, the third level Energy management system (brown color) is in charge of the optimal management of the DC microgrid, to satisfy the demand and maintain the balance of the system operating at minimum cost.

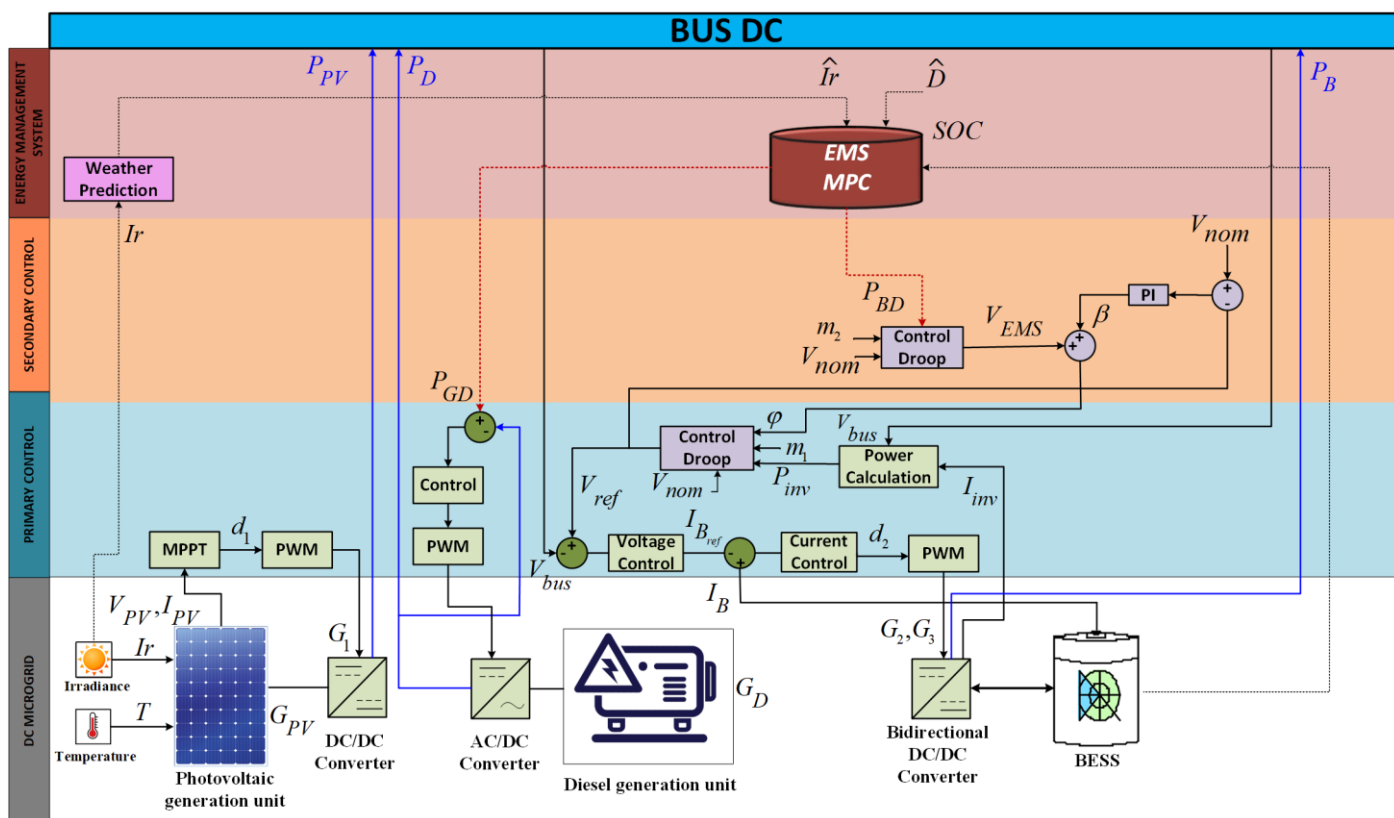


Figure 2. Control architecture.

As can be seen, photovoltaic generation unit the control requires a primary control, while the battery control contains a primary control and a secondary control, which allows the operation in charge and discharge mode of the BESS. The diesel generator as well as the battery when operating in discharge mode are dispatchable units, therefore, they have the characteristic of receiving the order from the EMS of the power to be delivered. Each level of control mentioned above is detailed in the following sections.

3.1. MPPT Control Strategy for the Photovoltaic System

The sun is a renewable and inexhaustible resource that produces energy, which can be collected and converted into heat (thermal energy) or electricity (photovoltaic energy) to meet the electricity demand [28].

Photovoltaic panels do not fully supply conventional loads, due to low voltage levels and low efficiency. Therefore, efficient control systems are needed to maximize the use of renewable resources. The objective is to develop and implement a control strategy, to achieve maximum power point tracking (MPPT) of the photovoltaic array, using a DC/DC Boost converter [29,30,31].

For the MPPT control, it is necessary to feed back on the voltage V_{PV} and current I_{PV} of the photovoltaic panel to calculate the maximum power point, finally, the PWM will generate the triggers to the gate pulse G_1 of the IGBTs to proceed to its activation. Allowing to obtain the voltage to be connected to the Bus DC of the microgrid see Figure 3.

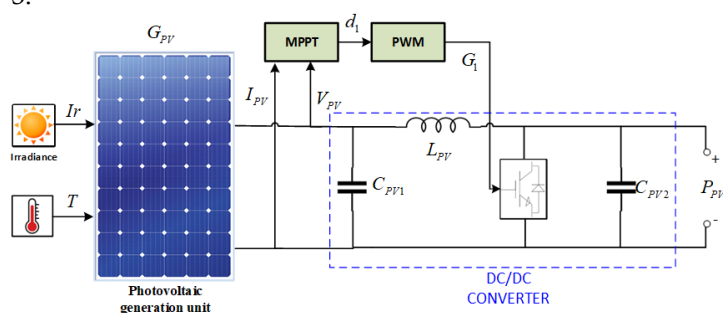


Figure 3. Control design for the photovoltaic system.

The important parameters used for an MPPT are irradiance and temperature since they directly affect the amount of electricity a photovoltaic panel can produce. In Figure 4, the maximum power operating point is shown by the characteristic curve of the photovoltaic panel. Figure 4a shows the relationship between current and voltage, while Figure 4b shows the relationship between power and voltage [29].

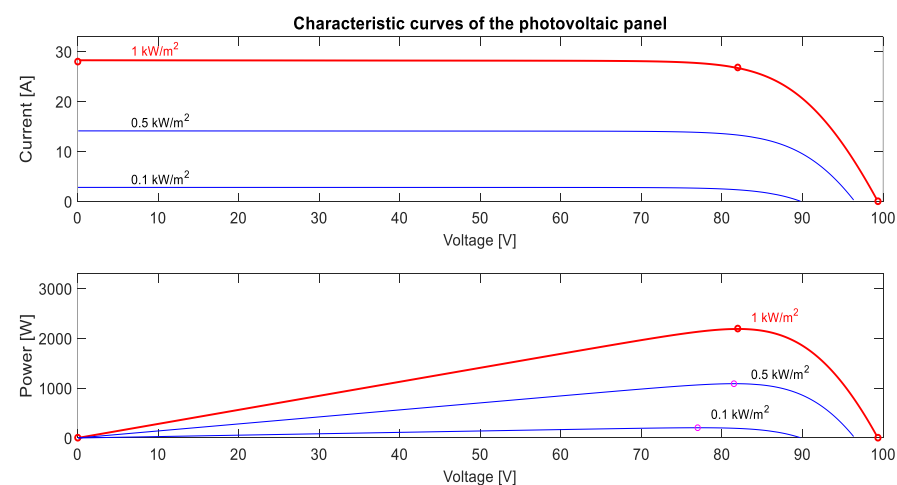


Figure 4. Characteristic curves of the photovoltaic panel: (a) I-V curve; (b) P-V curve.

Several algorithms allow obtaining the MPPT, this case, the incremental conductance algorithm was selected, for easy implementation and lower computational cost. This control technique is the most widely used because it can quickly calculate the maximum power point, in the face of disturbances due to rapidly fluctuating weather conditions [32].

According to [29] and [33] the incremental conductance algorithm (INC), is based on the slope of the power curve is zero in Equations (1) and (2) [34]. To begin with, the algorithm measures the voltage and current changes of the solar panels at a current time, and then compared them with the previous cycle measurements to predict the effect of a voltage change, to achieve the (MPP) it must be fulfilled that the rate of change in the output conductance $\frac{dI_{PV}}{dV_{PV}}$ is equal to the negative of the instantaneous conductance $\frac{I_{PV}}{V_{PV}}$ as in Equation (3),(4). This algorithm can follow irradiance changes faster than the perturbation and observation (P&O) algorithm for this reason it requires more complexity in its calculations, also according to [34] when the null derivative condition rules out steady-state oscillations.

$$\frac{dP_{PV}}{dV_{PV}} = 0 \quad (1)$$

Given that $P_{PV} = V_{PV} * I_{PV}$

$$\frac{d(V_{PV} * I_{PV})}{dV_{PV}} = 0 \quad (2)$$

$$I_{PV} + V_{PV} \frac{dI_{PV}}{dV_{PV}} = 0 \quad (3)$$

$$\frac{dI_{PV}}{dV_{PV}} = -\frac{I_{PV}}{V_{PV}} \quad (4)$$

Where: dP_{PV} is the derivative of the power photovoltaic panel, dV_{PV} is the derivative of the photovoltaic panel voltage, dI_{PV} is the derivative of the photovoltaic panel current, I_{PV} is the photovoltaic panel current, and V_{PV} is the photovoltaic panel voltage. When this is not satisfied, the points around the maximum point expressed in Equations (5) and (6) are analyzed [33].

$$Si \frac{dI_{PV}}{dV_{PV}} > -\frac{I_{PV}}{V_{PV}}, then \frac{dP_{PV}}{dV_{PV}} > 0 \quad left \quad (5)$$

$$Si \frac{dI_{PV}}{dV_{PV}} < -\frac{I_{PV}}{V_{PV}}, then \frac{dP_{PV}}{dV_{PV}} < 0 \quad right \quad (6)$$

Next, Figure 5 below shows the implemented incremental inductance scheme, and its output will be the control signal for the PWM control that will go to the IGBT G_1 .

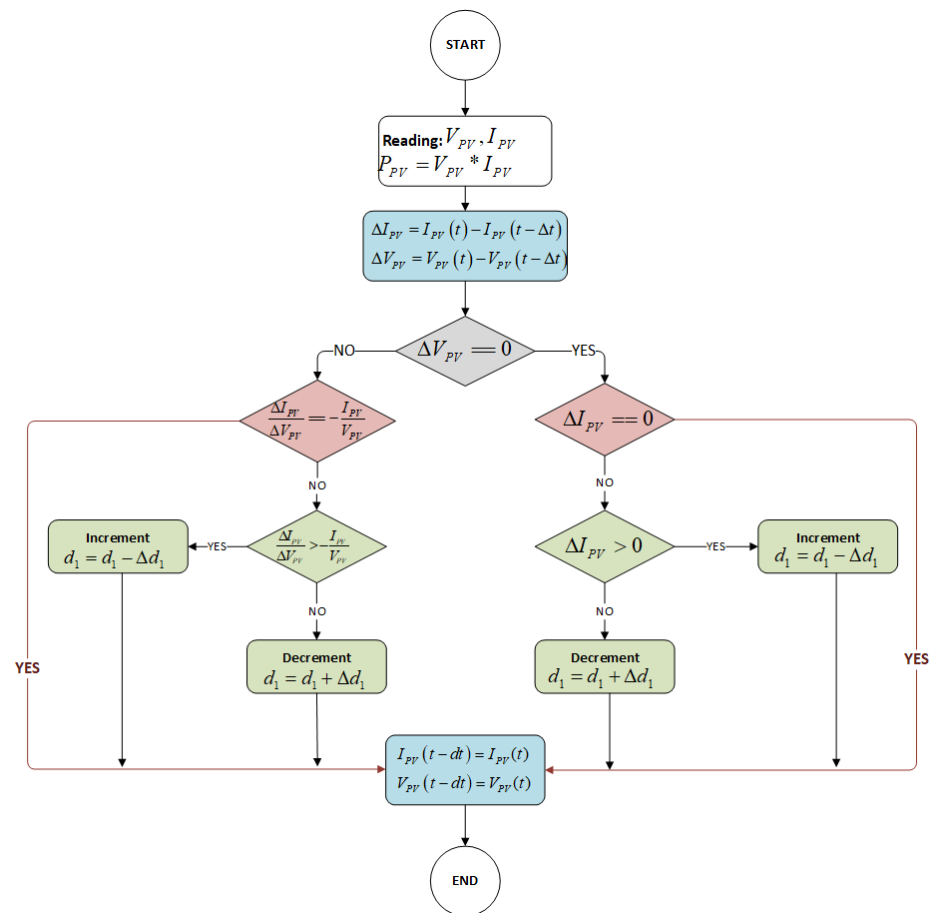


Figure 5. Diagram of the MPPT incremental conductance algorithm.

3.2 Local Control Strategy for the Storage System

The local control of the battery is responsible for keeping the generation levels regulated and avoiding deviations from the basic parameters in the power converters. This level of control is the fastest because it acts locally on the controls of the generation units, it's purpose is to maintain the voltage and current within the limits [35]. For local control of the storage system, a bidirectional DC/DC converter is implemented, used for energy storage applications where the ability to transfer energy in two directions is required. Since they seek to connect the battery for charge and discharge operation, therefore, they must be connected via a converter that allows both energy transfers [37].

That is why, in this research a "buck-boost" converter has been used, which is shown in Figure 6, working a Buck in BESS charging mode and Boost in discharging mode, depending on the control signal coming from the PWM regulated by the local voltage and current controllers see Figure 7, which generates the gate pulses G_2 and G_3 for the activation of the IGBT power switches [38,39,40].

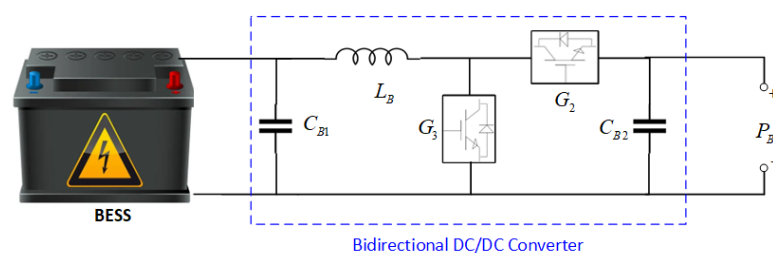


Figure 6. Bidirectional Converter "Buck-Boost"

The local controllers consist of: the proportional-integral (PI) voltage controller which maintains the voltage balance on the Bus DC, the PI current controller which is responsible for increasing or decreasing the amount of current depending on the demand, as well as the transition of the operating modes of the storage system, the PWM signal modulator will activate the IGBT switching elements, with the negated signal of the G_2 and the signal of the G_3 see Figure 7 [32,39].

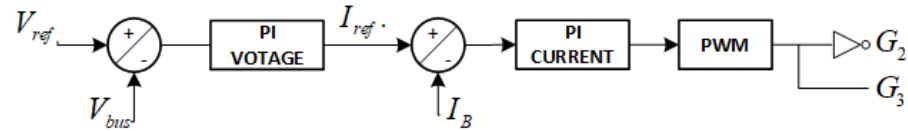


Figure 7. Control strategy for the storage system.

The cascade control of voltage and current is shown in Figure 7. The voltage controller regulates the battery voltage by maintaining the Bus DC voltage at a constant value, and the current control determines the mode of operation, in both charge and discharge modes. V_{ref} is the droop control output reference voltage, V_{bus} is the measured Bus DC voltage, I_{ref} is the reference current of the voltage PI controller output, I_B is the battery current measurement, and G_2 , and G_3 represent the IGBT triggers to the DC/DC converter. C_{B1} , and C_{B2} is the storage system DC/DC converter capacitors, L_B is the converter inductor, PI is proportional integral control.

To share power between different generation units, droop control is required, which is part of the primary control.

3.3 Droop control voltage – power

Voltage droop control is a conventional method, used for the ability to connect multiple generating units and distribute the power. Droop control is expressed in (7).

$$V_{ref} = V_{nom} - m_1 * P_{inv} \tag{7}$$

$$m_1 = \frac{\Delta V_{max}}{P_{max}} \tag{8}$$

$$\Delta V_{max} = V_{nom} - V_{min} \tag{9}$$

Where V_{ref} is the Droop control output, V_{nom} is the nominal DC microgrid voltage, m_1 is the Droop control coefficient, and P_{inv} is the inverter filter output power.

In (8) the relationship between the maximum acceptable voltage variation ΔV_{max} and P_{Bmax} is maximum power of the BESS. The ΔV_{max} is obtained in (9), and the V_{min} is 5% of the nominal voltage V_{nom} .

3.4 Secondary Control Strategy for the Storage System

The voltage restorer corrects the deviations caused by the primary control using a PI controller Figure 8 to maintain a constant voltage on the Bus DC. Where V_{nom} is going to be the desired voltage on the Bus DC and V_{ref} is the output of the droop control, and β is the control action [7,41].

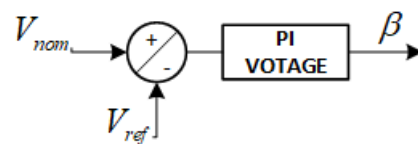


Figure 8. Voltage restorer secondary control strategy.

Equation (7) is modified by the secondary control action β to restore voltage and equation (10) is obtained, β corresponds to the secondary control action that allows voltage restoration see Figura 8.

$$V_{ref} = V_{nom} - m_1 * P_{inv} + \beta \quad (10)$$

Finally, the tertiary control or EMS sends the power to charge and discharge the battery, this power to be included in the lower levels of control is transformed into voltage for which the droop equation (11), is used, the same that as input the reference power of the droop P_{BD} . In this way, the output V_{EMS} is incorporated into (10), and equation (12). is obtained. Where V_{EMS} corresponds to the voltage delivered by the EMS control level for the optimum management of the microgrid.

$$V_{EMS} = V_{nom} - m_2 * P_{BD} \quad (11)$$

$$V_{ref} = V_{nom} - m_1 * P_{inv} + \beta + V_{EMS} \quad (12)$$

The description of predictive controller used for optimal microgrid management is described in the following section.

3.5 Optimal energy management

An energy management system (EMS) is in charge of managing the operation of the microgrid and energy demands, allowing it to satisfy the energy balance in a system [42].

For this research, a MPC strategy is proposed, which allows the optimal control of energy flow in a microgrid. This is based on the optimization of an objective function, using a mathematical model, the prediction model predicts the future state of the system and calculates the optimal control solution. Providing online control without the need for the implementation of a preset control law as in traditional control systems [42].

According to [42] and [16] the advantages offered by MPC control are:

- It can compensate for dead time.
- It compensates for measurable disturbances.
- The control law is easy to implement.
- It works the constraints in a systematic and conceptually simple way.

The optimizer provides the optimal inputs of the MPC by minimizing the objective function or also known as the cost function. The outputs are predicted by the mathematical model that takes the past signals (input and output signals) and the future signals as shown in Figure 9 [42].

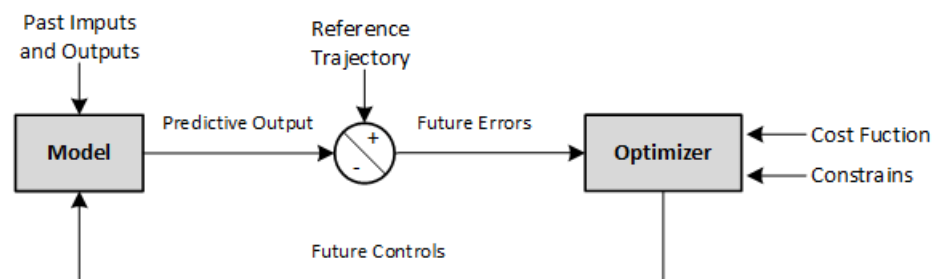


Figure 9. MPC Control Schematic.

The generation units require modeling to predict their status, which is described below.

3.5.1 Objective Function

The objective function implemented in the EMS system is defined by (13), to solve the optimal dispatch of the microgrid. The objective function minimizes the operating cost of the microgrid because the generation of energy based on fossil fuel is the only resource

that has a cost; therefore, it is necessary to minimize its consumption. Ade-more mini- 377
 mizes the unsupplied power and thus guarantees the supply of the demand. Where t rep- 378
 resents the samples and i the prediction horizon. 379

$$\min_{P_{GD}, P_{NS}, P_{BC}, P_{BD}, X_{GD}, X_{BC}, X_{BD}} \sum_{t=1}^i [P_{GD}(t) * cost_{GD} + P_{NS}(t) * cost_{NS}] \quad (13)$$

Where: P_{GD} is diesel generation power calculated by the EMS, P_{NS} represents the 380
 power not supplied, $cost_{GD}$ is cost of diesel power generation and the cost of unsupplied 381
 power is defined by $cost_{NS}$. 382

As the system evolves, t is increased sequentially, so the EMS input data is periodi- 383
 cally updated and therefore the optimization problem is updated with the new infor- 384
 mation obtained and the solutions are calculated, allowing the control system to be able 385
 to compensate for any perturbation. 386

The optimization variables are expressed as $P_{GD}, P_{NS}, P_{BC}, P_{BD}, X_{GD}, X_{BC}$ y X_{BD} . Where 387
 P_{BC} is battery charging power calculated by the EMS, P_{BD} is battery discharge power 388
 calculated by the EMS, X_{GD} represents the activation status of the diesel generator, while 389
 X_{BC} is the binary variable of the activation status of the battery charge mode and X_{BD} is 390
 the binary variable of the battery discharge mode activation state. 391

It is important to mention that the energy dispatch priority is focused first on renew- 392
 able energies that do not present operating costs, then on the BESS, and finally on the 393
 diesel generation unit in the case of not being able to meet the demand. It is therefore, is 394
 important to maintain the balance between voltage, power, and energy (produced, con- 395
 sumed, and stored). The optimization problem is subject to the constraints of the mi- 396
 crogrid, described below. 397

3.5.2 Constraints and Models of System 398

To solve the optimization problem, the following equation and inequality constraints 399
 are considered for the process, as described below. 400

Balance Condition 401

The microgrid needs to satisfy the balance equation, therefore, the power supplied 402
 by the generation units must be equal to the demand, which is analytically represented 403
 by equation (14). 404

Where the generation units are diesel generation power calculated by the EMS 405
 (P_{GD}), photovoltaic power (P_{PV}), battery discharge power calculated by the EMS (P_{BD}), 406
 unsupplied power (P_{NS}), battery charge power calculated by the EMS (P_{BC}) and the 407
 electrical demand as D . 408

$$D(t) - P_{NS}(t) - P_{BC}(t) = P_{GD}(t) + P_{PV}(t) + P_{BD}(t) \quad (14)$$

Diesel Generator Constraints 409

The power of the diesel generator must be kept within the generation limits accord- 410
 ing to its technical characteristics, which is represented by the inequality constraints de- 411
 fined in Equation (15). Where the binary variable X_{GD} is the binary variable of the activa- 412
 tion status of the diesel unit. Equation (15) corresponds to the power limits that the diesel 413
 generator unit can deliver, where P_{GDmax} is the maximum diesel power and P_{GDmin} is the 414
 minimum diesel power. 415
 416

$$P_{GDmin} * X_{GD}(t) \leq P_{GD}(t) \leq P_{GDmax} * X_{GD}(t) \quad (15)$$

BESS constraints

The modeling of the BESS is shown by Equations (16) and (17). Where Equation (16) represents the initial condition and Equation (17) is used to represent the energy of the BESS for any instant of time.

$$E(t) = E_0 + n_{BC} * P_{BC}(t) - \frac{P_{BD}(t)}{n_{BD}} \quad (16)$$

$$E(t) = E(t-1) + n_{BC} * P_{BC}(t) - \frac{P_{BD}(t)}{n_{BD}} \quad (17)$$

Where: $E(t)$ is instantaneous of the BESS power, E_0 is the initial energy of the BESS, n_{BC} is the BESS performance in charging mode, n_{BD} BESS performance in discharging mode. While $E(t-1)$ represents BESS energy at the previous instant.

Equation (18) defines the boundary constraint of the BESS based on the SOC, to keep the BESS within the safe operating threshold prolonging the lifespan. Where SOC_{max} represents upper charge limit of the BESS and SOC_{min} lower discharge limit of the BESS.

$$SOC_{min} \leq SOC(t) \leq SOC_{max} \quad (18)$$

To ensure that the charging and discharging of the BESS do not occur simultaneously, constraint (19) is added.

The power limits of the storage system are also capacity constraints which are described in equations (20), (21), and (22) for charging and discharging respectively. Where P_{Bmax} represents the maximum power of the BESS.

$$X_{BC}(t) + X_{BD}(t) \leq 1 \quad (19)$$

$$0 \geq P_{BC}(t) \geq -(P_{Bmax}) * X_{BC}(t) \quad (20)$$

$$0 \leq P_{BD}(t) \leq (P_{Bmax}) * X_{BC}(t) \quad (21)$$

$$E(t) \leq P_{Bmax} \quad (22)$$

Modeling of solar panels

The model designed in the MPC controller for the photovoltaic panels is defined by Equation (23).

$$P_{PV}(t) = n_{PV} * n_{inst} * A_t * Ir(t) \quad (23)$$

Where: n_{PV} photovoltaic panel performance, n_{inst} photovoltaic panel installation performance, A_t the total area of the panel array, and Ir the irradiance.

It is important to mention that the irradiance vector with dimension i is input to the EMS optimization problem as shown in Figure 2 and corresponds to the output of a prediction model. For the developed research it is taken into consideration that the solar resource is a time series, which is generated by a predictor model reported in [43].

4. Result

For this research, we propose an Energy Management System based on a MPC control for a DC microgrid in island mode with real-time measurement feedback for which the controls at the lower levels are implemented. The performance of the microarray without and with EMS is compared.

The microgrid consists of a photovoltaic generation unit, BESS, and diesel generation unit connected to a Bus DC with the corresponding power electronics interfaces to supply

a DC load as shown in Figure 1. The models of the generation units and controllers designed at the different control levels described in sections 3-4 are simulate in Matlab/Simulink software. For the design and simulation of the proposed optimization problem, the Fico Xpress Optimization software is used, linking the two software to emulate a real operation where the supervisory control for the microgrid management sends and receives signals from the microgrid operation. The simulation parameters used for the microgrid are described in Tables 1-4. The photovoltaic generation unit operating parameters, BESS parameters, and diesel generator unit parameters are shown in Tables 1, 2, and 3, respectively, while the converter and load parameters are shown in Table 4.

Table 1 Photovoltaic panel parameters.

Description	Parameter	Value
Array tension panel	V_{oc}	49.68 V
Maximum power array voltage	V_{mp}	40.98 V
Array current panel	I_{sc}	14.01 A
Maximum power array current	I_{mp}	13.42 A

Table 2. BESS parameters

Description	Parameter	Value
Voltage	V	36 V
Ampere-Hour	Ah	10 Ah
Conditions Initial Charge State	SOC (%)	75 %
The upper limit of a state of charge	SOC _{max}	90%
The lower limit of discharge state	SOC _{min}	40%

Table 3. Characteristics of the Diesel Generator.

Description	Parameter	Value
Minimum diesel power	$P_{GD_{min}}$	600 W
Maximum diesel power	$P_{GD_{max}}$	6000 W
Cost diesel	$cost_{GD}$	\$0.046 USD /lt

Table 4. Characteristics of the converters.

Description	Parameter	Value
Photovoltaic capacitor 1	C_{PV1}	1800 μF
Photovoltaic capacitor 2	C_{PV2}	18000 μF
Photovoltaic inductor	L_{PV}	1.7 mH
Capacitor 1 battery	C_{B1}	390.63 μF
Capacitor 2 battery	C_{B2}	390.63 μF
Battery inductance	L_B	9 mH
Nominal voltage of Load	V_{nom}	48 V

4.1 Evaluation of DC microgrid operation

This section validates the performance of the DC microgrid. The following scenarios are analyzed and compared: i) without considering the optimal management of the EMS,

only with the primary controls ii) considering the optimal management of the proposed EMS, which includes real-time feedback of the measured variables, the EMS is operating in sliding mode, i.e. it takes samples every 5 seconds and recalculates the optimal solutions for the control of the microgrid. The microgrid is subject to disturbances from changes in radiation and also changes in demand. The microgrid's performance is analyzed in terms of technical, economic, and optimal battery management.

Figures 12 - 13 show the results obtained by applying the radiation profile (Figure 10) and demand changes (Figure 11) for the scenarios with and without EMS. The radiation profile ranges from 400 W/m² to a maximum irradiance of 900 W/m² at different time intervals.

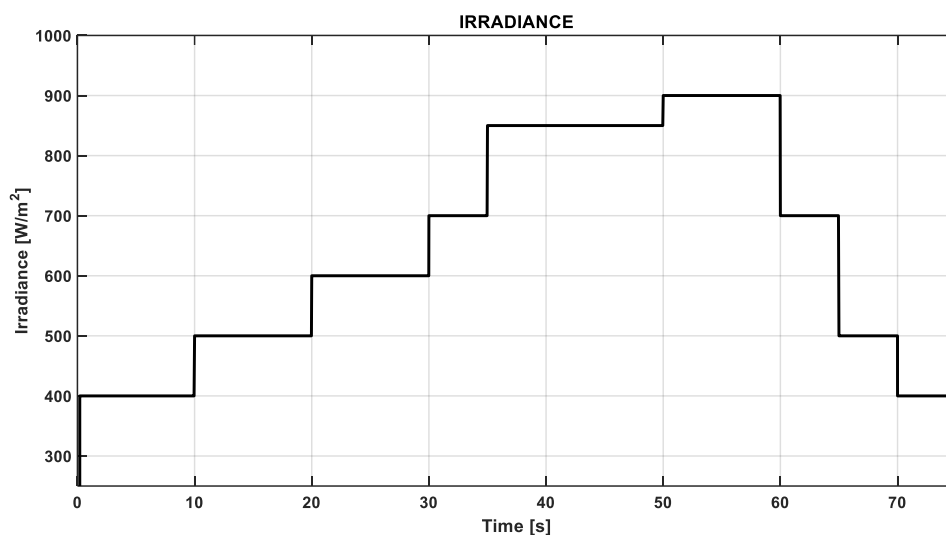


Figure 10. Irradiance profile.

Given the radiation profile proposed in Figure 10 and the demand profile as shown in Figure 11.

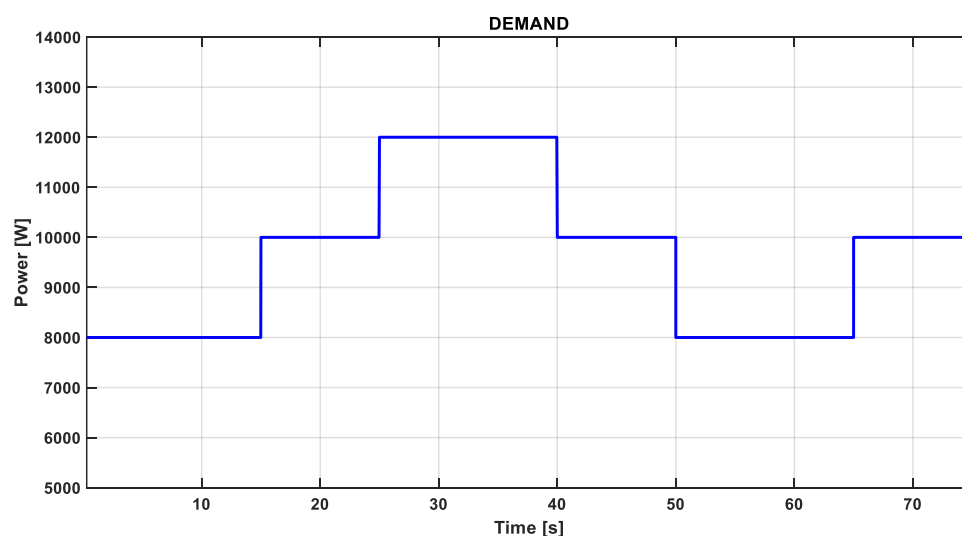


Figure 11. Demand profile.

Figure 12 shows the performance of the DC microgrid. Figure 12a shows the active power distribution when operating with the proposed EMS, this information is also visible in Table 5. During the time interval from 0 to 10 seconds to supply the demand, the photovoltaic panels deliver their maximum power (red line), which is not enough to meet the power balance, so the EMS resolves that the optimal dispatch is that the battery enter with

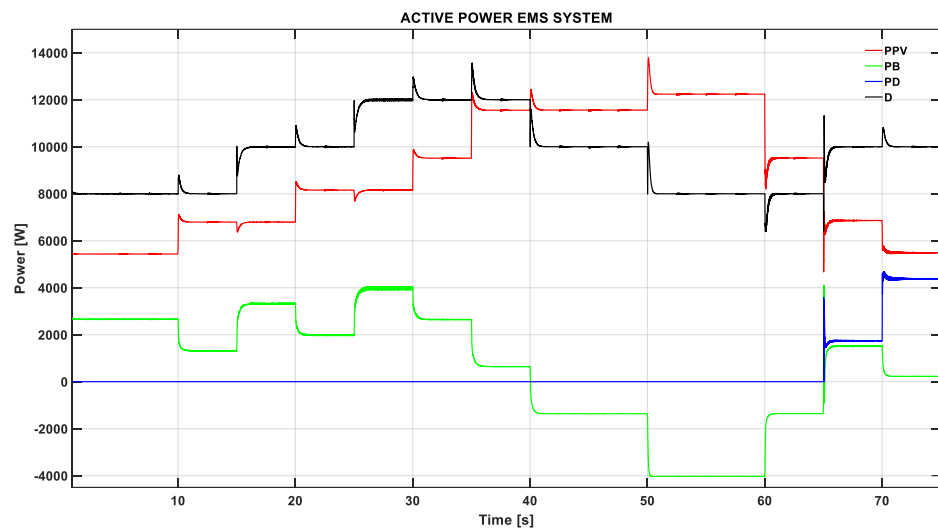
the remaining power (green line) to meet the demand (black line). In addition, after 5 seconds the controller is run again with the updated inputs and measurements and it can be noted that there is no change in the power distribution. At 10 seconds there is an increase in radiation and it is shown how the battery reduce the power generated to take advantage of the natural resource, at 15 seconds there is an increase in demand of 10000 W, and since the solar power remains equal to the previous operating point the battery support to meet the power balance, in the interval from 20 to 40 seconds there is a variation of demand and solar power, however, the demand is always higher, which leads to the battery to deliver the necessary missing power to meet the balance of power. In the time intervals from 40 to 65 seconds, it can be noticed that the photovoltaic power is higher than the power required by the demand, and with the objective of not wasting the natural resource the battery start to charge therefore they present a negative power, i.e. the battery becomes a load of the microgrid. However, as shown in Figure 12b in the intervals from 40 to 65 the battery fails to be fully charged and does not reach the upper limit of the SOC (90%), so in the second 65 when the solar power is reduced and the demand increases, the battery delivers according to its discharge capacity.

In the second 65 the solar power is reduced and the electrical demand increases, this is supplied by the solar power with 6810W plus the power generated by the battery which is not fully charged so it delivers according to its discharge characteristics 1450W, therefore, it is not enough to meet the balance of powers, so the EMS integrates the Diesel generator (blue line) that supports with 1740 W, to supply the demand. Finally, after 70 seconds the solar power is reduced, and the diesel generator must increase its supply.

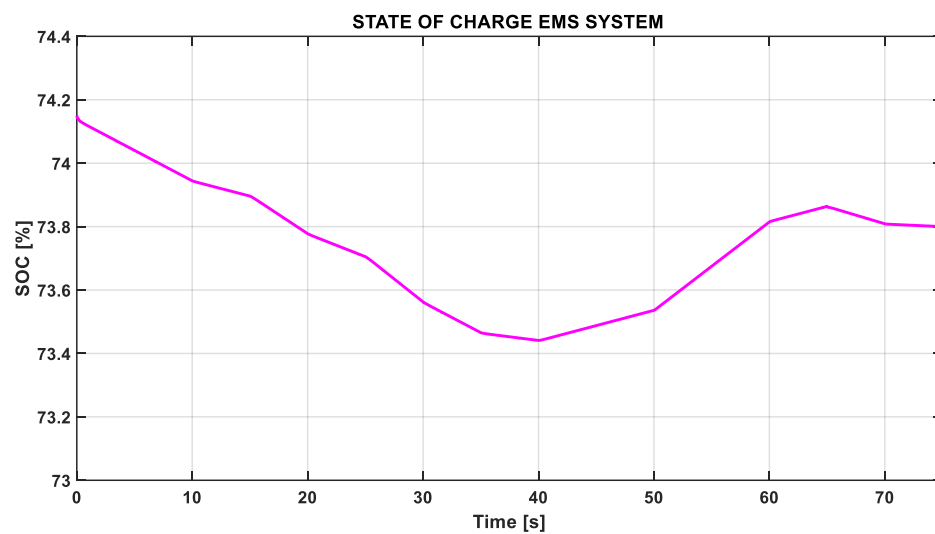
The operating costs produced by the diesel generator in the period time of 60 to 65 seconds is \$0.00056 USD and during 70 to 75 seconds is \$0.0014 USD, with a total operating cost of \$0.002 USD. Taking into consideration that the commercial cost of diesel in Ecuador is \$0.0462 USD/lit.

Table 5. Active Power microgrid with EMS.

Item	Time [s]	P_{PV} [W]	P_B [W]	P_D [W]	D[W]
1	0-5	5395	2605	0	8000
2	5-10	5395	2605	0	8000
3	10-15	6720	1280	0	8000
4	15-20	6720	3280	0	10000
5	20-25	8127	1873	0	10000
6	25-30	8127	3873	0	12000
7	30-35	9483	2517	0	12000
8	35-40	11452	548	0	12000
9	40-45	11452	-1452	0	10000
10	45-50	11452	-1452	0	10000
11	50-55	12059	-4059	0	8000
12	55-60	12059	-4059	0	8000
13	60-65	9317	-1317	0	8000
14	65-70	6810	1450	1740	10000
15	70-75	5448	251	4301	10000



(a)



(b)

Figure 12. Microgrid performance with EMS (a) Active Power Microgrid y (b) SOC of-BESS.

Figure 13 shows the microgrid's performance without EMS. Figure 13a shows the distribution of active power by the generation units of the microgrid, without including the optimal EMS dispatch, this information is also visible in Table 6, during the interval from 0 to 15 seconds the demand (black line) is satisfied by the solar generation (red line) and the battery (green line), without the intervention of the diesel generator (blue line). In addition, in the second 15, there is an increase in demand of 10000 W, the solar power remains the same as the previous operating point and it can be noticed how the battery continues to discharge, however, the diesel generator also starts to deliver a power of 2000 W. In the second 20, the solar power increases to 8127 W, but with a demand equal to the previous interval, however, the diesel generator continues to generate 2000 W, unlike the operation with EMS (Figure 12a) in this interval the diesel generator remains off. The operation of the microgrid in the interval from 25 to 40 seconds shows that the demand is higher than the solar power, in addition, the diesel generator keeps delivering the same power of the previous interval, which does not happen in the scenario with EMS since this control calculates the power distribution at a minimum cost reducing the use of the diesel generator, In the time interval from 40 to 65 seconds the demand is completely supplied by the solar power and since the solar energy is higher than the demand, the surplus energy is stored

525
526527
528
529
530
531532
533
534
535
536
537
538
539
540
541
542
543
544
545
546
547
548

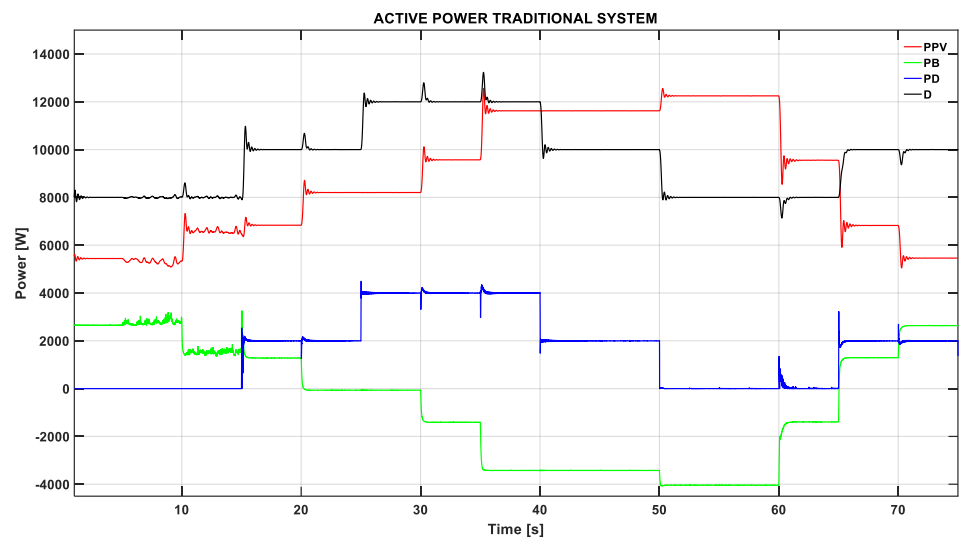
in the battery which have negative power, i.e. it becomes a load of the microgrid. Finally in the last time interval from 65 to 75 seconds, the demand increases to 10000 W and the photovoltaic power is reduced, in addition, to supplying the demand the diesel unit delivers 2000 W because there is no controller to properly manage the power, it can be observed that despite there is a variation of photovoltaic power the diesel generator delivers a constant power, In comparison with the EMS, it can be observed that in this same time interval, the diesel power is distributed since between 65 to 70 seconds and 70 to 75 seconds the photovoltaic power is different so the EMS recalculates and gives the order to the diesel generator to supply the missing power for each case, supplying the demand.

Figure 13b shows how from 20 seconds the battery start with their charging process because the diesel generator starts to supply the missing power to the demand, however, this is not the most economical way to operate the microgrid due to fuel consumption and environmental pollution, despite this the battery are not fully charged to their maximum point, so in the second 65 when the solar power is reduced and the demand increases, the battery delivers according to its discharge capacity.

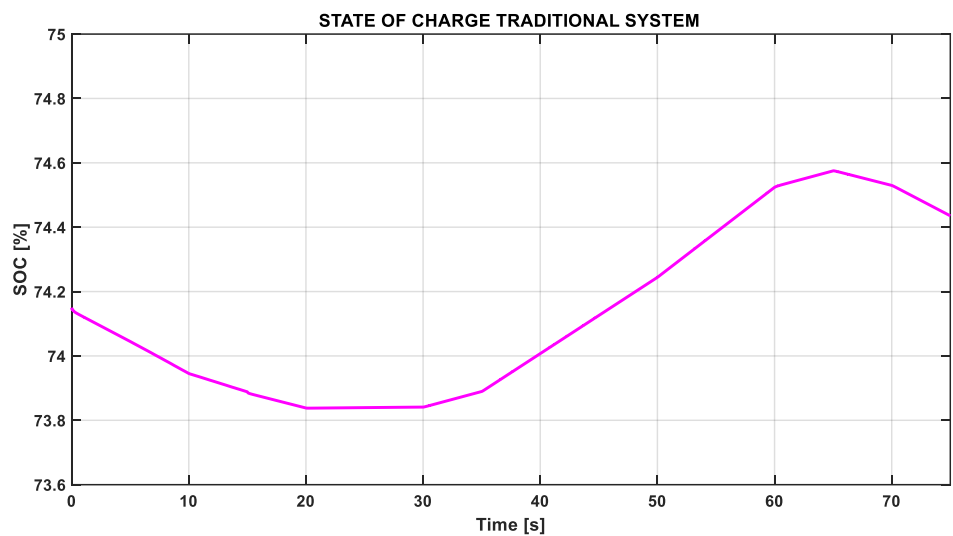
The cost of operating the diesel generator without an EMS during the periods of 15 to 25, 40 to 50, and 65 to 75 seconds is \$0.00064 USD respectively, and in the time interval of 25 to 40 seconds, the cost generated is \$0.00128 USD, giving a total cost of generation of \$0.0077 USD.

Table 6. Active Power microgrid without EMS.

Item	Time [s]	$P_{PV}[W]$	$P_B[W]$	$P_D[W]$	D [W]
1	0-5	5395	2605	0	8000
2	5-10	5395	2605	0	8000
3	10-15	6720	1280	0	8000
4	15-20	6720	1280	2000	10000
5	20-25	8127	-127	2000	10000
6	25-30	8127	-127	4000	12000
7	30-35	9483	-1483	4000	12000
8	35-40	11452	-3452	4000	12000
9	40-45	11452	-3452	2000	10000
10	45-50	11452	-3452	2000	10000
11	50-55	12059	-4059	0	8000
12	55-60	12059	-4059	0	8000
13	60-65	9317	-1317	0	8000
14	65-70	6810	1190	2000	10000
15	70-75	5448	2552	2000	10000



(a)



(b)

Figure 13. Microgrid performance without EMS (a) Active Power Microgrid y (b) SOC of BESS.

Implementing the EMS tertiary control working in sliding mode allows us to calculate the optimal solutions for the distribution of power in the microgrid as shown in Figure 12a, through real-time measurements of the variables, it is shown that in most of the simulation period, the diesel generator remains deactivated, to minimize costs, This means that the control algorithm does not activate the auxiliary unit, which is reflected in the reduction of operating costs and reduction of environmental pollution, in addition to extending the life of the battery, preventing them from operating at critical points such as overloads or deep discharges, while complying with the power balance to supply the required demand. While the system without EMS shown in Figure 13a, supplies the demand, since it does not have the optimal power flow management, the power distribution between the supply units and the battery is not efficient, which is why in the simulation time the diesel unit supplies energy most of the time, in addition, it does not take care of the operation of the battery because they present deep discharges.

5. Conclusions

This paper presents the design of the primary, secondary, and tertiary controllers for a DC microgrid in island operation. The tertiary control (EMS) allows optimal microgrid management, ensuring optimal power distribution and protecting the lifespan of the battery, using real-time measurement feedback that allows it to react to rapid changes in electrical demand and radiation changes. The primary level corresponds to the voltage and current control for the battery to work in charge and discharge mode, while the photovoltaic power includes an MPPT control based on the incremental conductance algorithm, to take full advantage of the solar resource. In addition, this level includes a Droop Control to perform the power-sharing of the battery. However, this action causes a deviation in the operating voltage of its nominal value, so a second level of control is implemented to restore voltage. Finally, in the third level of control, an EMS is implemented to determine the power of each generating unit must deliver to cover the demand while complying with the technical operating constraints and protecting the lifespan of the battery.

The implemented EMS detects disturbances occurring at lower control levels and operates in the face of rapid changes in radiation and electrical demand. Measurements of battery status and available energy are feedback online by the EMS, and predictions are updated. Thus, the optimal decision of battery usage is more efficient, and the algorithm considers battery operating limit constraints to avoid deep discharges.

The EMS reduces the operating cost by 40% compared to the microgrid without the optimal management system in the evaluating horizon by reducing fuel consumption to supply the demand.

In this research work, the optimal performance of the DC microgrid has been validated by evaluating all levels of control, guaranteeing optimal operation in technical terms, i.e. the use of the natural resource, and economic terms by obtaining the minimum operating cost and protecting the lifespan of the battery.

The proposed EMS respects the established SOC limits, therefore, it does not reach deep discharges and mainly presents an optimal operation where the charge and discharge decisions are made by the EMS, i.e., they are taken according to the availability of the natural resource and the minimum cost for the DC microgrid.

Having the design and implementation of the three levels of control allows for identifying the impact that each level has on the EMS and how the disturbances affect the optimal operation. That is why, in our proposal, EMS, by updating the measurements that represent the short-term inputs, can respond to changes detected in the lower levels of control, i.e., when disturbances occur, therefore the operation of the DC microgrid is integral.

It is determined as future work that within the optimization problem we can add the restrictions of the diesel generator start-up time, and modeling of the battery degradation, in addition, we can include the modeling and restriction of the electrical network connected to the microgrid allowing to increase the energy supply capacity of the system. From the control point of view, our main future work will focus on a comparison between a centralized and a distributed system of DC microgrids.

Nomenclature

A_t	Total area of the panel array
Ah	Ampere-Hour
AC	Alternating Current
IA	Artificial Intelligence
$BESS$	Battery Energy Storage System
CO_2	Carbon dioxide

C_{B1}, C_{B2}	Capacitors Battery
C_{PV1}, C_{PV2}	Photovoltaic Capacitors
$cost_{GD}$	Cost of diesel power generation
$cost_{NS}$	Cost of unsupplied power
D	Electrical demand
DC	Direct Current
$DMPC$	Decentralized Model Predictive Control
DSM	Demand Side Management
d_1, d_2	Duty cycle
dI_{PV}	Derivative of photovoltaic panel current
dP_{PV}	Derivative of photovoltaic panel power
dV_{PV}	Derivative of photovoltaic panel voltage
EMS	Energy Management System
$E(t)$	Instantaneous of the BESS power
$E(t - 1)$	BESS energy at the previous instant
E_0	Initial energy of the BESS
EV	Electric vehicles
G_D	Diesel generation unit
G_1, G_2, G_3	Gates pulses
G_{PV}	Photovoltaic generation unit
I_B	Battery current measurement
I_{sc}	Array current panel
I_{mp}	Maximum power array current
I_{PV}	Photovoltaic panel current
$I_{PV}(t)$	Photovoltaic current in instant
$I_{PV}(t - \Delta t)$	Photovoltaic current in a previous instant
I_{ref}	Reference current of the voltage PI controller output
INC	Incremental Conductance Algorithm
IGBT	Insulated Gate Bipolar Transistor
I_r	Irradiance
\hat{I}_r	Predicted Irradiance
i	Prediction horizon
L_B	Battery Inductance
L_{PV}	Photovoltaic Inductor
m_1, m_2	Droop Control Coefficients
MOGA	Multi-Objective Genetic Algorithm
MPC	Model predictive control
MPPT	Maximum Power Point Tracking
n_{BC}	BESS performance in charge mode

n_{BD}	BESS performance in discharge mode
n_{PV}	Photovoltaic panel performance
n_{inst}	Photovoltaic panel installation performance
NSGA – II	Non-Dominated Sorting Genetic Algorithm
P_B	Battery power
P_{Bmax}	Maximum power of the BESS
P_{BC}	Battery charging power calculated by the EMS
P_D	Diesel power
P_{BD}	Battery discharge power calculated by the EMS
P_{GD}	Diesel generation power calculated by the EMS
P_{GDmin}	Minimum diesel power
P_{GDmax}	Maximum diesel power
P_{NS}	Power not supplied
P_{PV}	Photovoltaic power
P_{inv}	Inverter Filter Output Power
P&O	Perturbation and observation algorithm
PI	Integral proportional controller
PWM	Pulse Width Modulation
SOC	State of charge
SOC_{max}	Upper charge limit of the BESS
SOC_{min}	Lower discharge limit of the BESS
SOC (%)	Conditions Initial Charge State
T	Temperature
t	Samples
V	Voltaje
V_{EMS}	Voltage delivered by the EMS
V_{PV}	Photovoltaic panel voltage
$V_{PV}(t)$	Photovoltaic voltage in instant
$V_{PV}(t - \Delta t)$	Photovoltaic voltage in a previous instant
V_{bus}	Measured Bus DC voltage
V_{min}	5% of de nominal voltage
V_{nom}	Nominal voltage of the microgrid
V_{ref}	Droop control output reference voltage
V_{oc}	Array tension panel
V_{mp}	Maximum power array voltage
X_{BC}	The Binary variable of the activation status of the battery charge mode
X_{BD}	The Binary variable of the battery discharge mode activation state

X_{GD}	The Binary variable of the activation status of the diesel unite
β	Secondary control action
ΔI_{PV}	Variation of photovoltaic panel current
ΔV_{PV}	Variation of photovoltaic panel voltage
Δd_1	Variation of Duty cycle
ΔV_{max}	Maximum Acceptable Voltage Variation

636

References

637

- FENERCOM, "Basic Guide to Distributed Generation," Madrid, Spain, 2017. [Online]. Available: <http://www.madrid.org/cs/Satellite?blobcol=urldata&blobheader=application/pdf&blobheadername1=Content-Disposition&blobheadervalue1=filename=GUIA+BASICA+DE+LA+GENERACION.pdf&blobkey=id&blobtable=MungoBlobs&blobwhere=1181215450713&ssbinary=true>. 638
- D. Á. Prats, R. A. García, and J. V. Alonso, "Hybrid systems based on renewable energies for power supply to desalination plants," *Mech. Eng.*, vol. 14, no. 1, pp. 22–30, 2011. 639
- K. A. Andrade Granja, "Optimal geographically distributed micro-grid management system to maximize energy sales based on demand response programs.," Salesian Polytechnic University, Quito, Ecuador, 2021. 640
- Rey, Juan M, Geovanni A Vera, Pedro Acevedo Rueda, Javier Solano, Maria A Mantilla, Jacqueline Llanos, and Sáenz Doris, "A Review of Microgrids in Latin America : Laboratories and Test Systems," *IEEE Lat. Am. Trans.*, vol. 20, no. 6, pp. 1000–1011, 2022. 641
- G. Barrales Alcaín, "Isolated Microgrids: A challenge for DSO's," School of Engineering (ICAI), Madrid, Spain, 2016. 642
- Quijano, Nicanor, Angélica Peraza, Miguel Velásquez, Estévez Jiménez, Ángela Cadena, Jorge Becerra, and Álvaro Ramírez, "Isolated Microgrids in La Guajira: Design and Implementation," *Engineering Magazine*, no. 48, p. 55, 2019. 643
- A. P. Moya, P. J. Pazmiño, J. R. Llanos, D. Ortiz-Villalba, and C. Burgos, "Distributed Secondary Control for Battery Management in a DC Microgrid," *Energies*, vol. 15, no. 22, pp. 1–20, 2022, doi: 10.3390/en15228769. 644
- M. Rodríguez, A. Salazar, D. Arcos-Aviles, J. Llanos, W. Martínez, and E. Motoasca, "A brief approach of Microgrids implementation in Ecuador: A review," vol. 1, pp. 149–161, 2021, doi: 10.1007/978-3-030-72208-1_12. 645
- F. Alex Navas, J. S. Gomez, J. Llanos, E. Rute, D. Saez, and M. Sumner, "Distributed predictive control strategy for frequency restoration of microgrids considering optimal dispatch," *IEEE Trans. Smart Grid*, vol. 12, no. 4, pp. 2748–2759, 2021, doi: 10.1109/TSG.2021.3053092. 646
- J. L. Proano, D. O. Villalba, D. Saez, and D. O. Quero, "Economic dispatch for optimal management of isolated microgrids," *2016 IEEE 36th Cent. Am. Panama Conv. CONCAPAN 2016*, pp. 2–7, 2016, doi: 10.1109/CONCAPAN.2016.7942382. 647
- J. I. López Torrez, "Energy storage systems from battery banks for the integration of renewable energy sources in DC microgrids.," Technological University of Pereira, Pereira, Colombia, 2015. 648
- M. Fotopoulou, D. Rakopoulos, D. Trigkas, F. Stergiopoulos, O. Blanas, and S. Voutetakis, "State of the art of low and medium voltage direct current (Dc) microgrids," *Energies*, vol. 14, no. 18, 2021, doi: 10.3390/en14185595. 649
- D. Duarte and B. Peñuela, "Análisis para la transición de microredes residenciales de corriente AC a corriente DC," Universidad de La Salle, 2020. 650
- M. El-Hendawi, H. A. Gabbar, G. El-Saady, and E.-N. A. Ibrahim, "Control y EMS de una microrred conectada a la red con análisis económico," *Energies*, p. 2, 2018, doi: 10.3390/en11010129. 651
- Navas-Fonseca, Alex, Claudio Burgos-Mellado, Juan S. Gomez, Jacqueline Llanos, Enrique Espina, Doris Saez, and Mark 652

669

- Sumner, “Distributed Predictive Control using Frequency and Voltage Soft Constraints in AC Microgrids including Economic Dispatch of Generation,” *IECON Proc. (Industrial Electron. Conf.)*, vol. 2021-October, no. i, 2021, doi: 10.1109/IECON48115.2021.9589500.
16. E. F. Camacho and C. Bordons, “Predictive Control: Past, Present and Future,” *Iberoam. J. Autom. Ind. Informatics*, vol. 1, pp. 5–28, 2004.
17. M. Saltos-Rodríguez, D. Ortiz-Villalba, J. Llanos, C. Chipantiza-Punguil, and G.-R. R, “Practical Framework for Optimal Planning of Microgrids for Production Processes,” *IEEE 36th Cent. Am. Panama Conv. (CONCAPAN XXXVI)*, pp. 4–11, 2016, doi: 10.1109/CONCAPAN.2016.7942382.
18. Palma-Behnke, Rodrigo, Carlos Benavides, Fernando Lanas, Bernardo Severino, Lorenzo Reyes, Jacqueline Llanos, and Doris Saez, “A microgrid energy management system based on the rolling horizon strategy,” *IEEE Trans. Smart Grid*, vol. 4, no. 2, pp. 996–1006, 2013, doi: 10.1109/TSG.2012.2231440.
19. E. E. Carvajal González, G. J. Muñoz López, and S. Rivera, “Optimization of microgrid operation considering operating cost, battery life and uncertainty cost of wind energy,” *Between Sci. Eng.*, vol. 13, no. 25, pp. 24–33, 2019, doi: 10.31908/19098367.4011.
20. C. Bordons, F. García Torres, and L. Valverde, “Optimal Energy Management in Microgrids with Renewable Generation,” *Iberoam. J. Ind. Autom. Informatics*, vol. 12, no. 2, pp. 117–132, 2015, doi: 10.1016/j.riai.2015.03.001.
21. A. Parisio and L. Glielmo, “Energy efficient microgrid management using Model Predictive Control,” in *Proceedings of the IEEE Conference on Decision and Control*, 2011, pp. 5449–5454, doi: 10.1109/CDC.2011.6161246.
22. F. A. Zuñiga Cortes, E. F. Caicedo Bravo, and D. M. López Santiago, “Optimal Electric Power Management in a Connected Microgrid, based on the Genetic Algorithm for Multiobjective Optimization MOGA,” *UIS Eng. Mag.*, vol. 15, no. 2, pp. 17–28, 2017, doi: 10.18273/revuin.v15n2-2016002.
23. R. Ignacio and B. Bustos, “Predictive Control for a Micro-Network Coordination system considering Demand Management,” University of Chile, Chile, 2022.
24. D. Trigkas, G. Gravanis, K. Diamantaras, S. Voutetakis, and S. Papadopoulou, “Energy Management in Microgrids Using Model Predictive Control Empowered with Artificial Intelligence,” *Chemical Engineering Transactions*, vol. 94, pp. 961–966, 2022.
25. C. Bordons, F. GarciaTorres, and M. A. Ridaou, “Predictive control in interconnected microgrids and with electric vehicles,” *Iberoam. J. Autom. Ind. Informatics*, vol. 17, no. 3, pp. 240–250, 2020, doi: 10.4995/riai.2020.13304.
26. K. Sayed, A. G. Abo-Khalil, and A. S. Alghamdi, “Optimum resilient operation and control DC microgrid based electric vehicles charging station powered by renewable energy sources,” *Energies*, vol. 12, no. 22, 2019, doi: 10.3390/en12224240.
27. J. A. Cuéllar Guarnizo, “Design of a Controller for Maximum Power Point Tracking (MPPT) in Solar Panels.,” University of Santo Tomás, Bogotá, Colombia, 2019.
28. R. A. Álvarez López and A. A. Manrique, “Implementation of Photovoltaic Generation as a Back-up for Distribution Grid Failures,” *Colombian Journal of Advanced Technologies (RCTA)*, vol. 2, no. 22, pp. 14–19, 2013.
29. H. Acevedo Meza, J. L. Mendoza García, and S. Sepúlveda Mora, “MPPT Control Strategies Applied in a DC/DC Boost Converter for PV Systems,” *Colomb. J. Adv. Technol.*, vol. 2, no. 30, pp. 102–107, 2017, doi: 10.24054/16927257.v30.n30.2017.2751.
30. S. Intriago, P. Robayo, J. Llanos, F. Silva, and J. Gómez, “Comparison of Control Strategies for Monitoring the Maximum Power Point Tracking of a Photovoltaic Plant,” *6th IEEE Ecuador Tech. Chapters Meet. ETCM 2022*, 2022, doi: 10.1109/ETCM56276.2022.9935710.
31. R. Cuzco, D. Arcos-Aviles, J. Llanos, D. Ortíz, and W. Martínez, “Comparative Analysis of the Performance of Maximum Power Point Tracking Algorithms in Photovoltaic Systems,” *XV Multidiscip. Int. Congr. Sci. Technol.*, vol. 931 LNEE, no. June, 2022.

- pp. 274–289, 2022, doi: 10.1007/978-3-031-08280-1_19. 712
32. A. El-Shahat and S. Sumaiya, “DC-microgrid system design, control, and analysis,” *Electron.*, vol. 8, no. 2, 2019, doi: 10.3390/electronics8020124. 713
714
33. N. Echeverría, M. Judewicz, G. Murcia, J. Strack, and S. González, “Incremental Conductance MPPT Algorithm with Double Peak,” *Aadeca*, no. September, p. 9, 2014, doi: 10.13140/2.1.2604.6720. 715
716
34. J. E. Vera, J. F. Bayona, and R. Sánchez, “Maximum power point tracking (SPMP) on solar panels,” *Vis. Electron.*, vol. 8, no. 2, pp. 50–53, 2014. 717
718
35. R. D. Medina, “Microgrids Based on Power Electronics: Part II: Active and Reactive Power Control,” *Ingenius*, no. 12, pp. 24–34, 2014, doi: 10.17163/ings.n12.2014.03. 719
720
36. M. D. Keshavarzi and M. H. Ali, “A Novel Bidirectional DC-DC Converter for Dynamic Performance Enhancement of Hybrid AC/DC Microgrid,” *Electron.*, vol. 9, no. 10, pp. 3–15, 2020, doi: 10.3390/electronics9101653. 721
722
37. J. M. Benot Morell, “Control of AC/DC and DC/AC converters for charging electric vehicles,” University of Seville, Spain, 2012. 723
724
38. J. Posada Contreras, “Pulse width modulation (PWM) and vector modulation (SVM). An introduction to modulation techniques,” *Lat. Am. Netw. Sci. Journals*, vol. 1, pp. 70–80, 2005, [Online]. Available: <http://www.doaj.org/doi?func=abstract&id=256164>. 725
726
727
39. J. Lv, X. Wang, G. Wang, and Y. Song, “Research on control strategy of isolated dc microgrid based on soc of energy storage system,” *Electron.*, vol. 10, no. 7, 2021, doi: 10.3390/electronics10070834. 728
729
40. Y. Alidrissi, R. Ouladsine, A. Elmouatamid, R. Errouissi, and M. Bakhouya, “Constant Power Load Stabilization in DC Microgrids Using Continuous-Time Model Predictive Control,” *Electron.*, vol. 11, no. 9, 2022, doi: 10.3390/electronics11091481. 730
731
732
41. J. Llanos, J. Gomez, D. Saez, D. Olivares, and J. Simpson-Porco, “Economic dispatch by secondary distributed control in microgrids,” *21st Eur. Conf. Power Electron. Appl. EPE 2019 ECCE Eur.*, no. December, pp. 1–10, 2019, doi: 10.23919/EPE.2019.8915499. 733
734
735
42. S. Ruiz Moreno, “Energy management of a Microgrid through Model Predictive Control,” University of Sevilla, Sevilla, Spain, 2019. 736
737
43. J. A. Segovia, J. F. Toaquiza, J. R. Llanos, and D. R. Rivas, “Meteorological Variables Forecasting System Using Machine Learning and Open-Source Software,” *Electronics*, 2023, [Online]. Available: <https://doi.org/10.3390/electronics12041007>. 738
739
44. S. U. Ali, A. Waqar, M. Aamir, S. M. Qaisar, and J. Iqbal, “Model predictive control of consensus-based energy management system for DC microgrid,” *PLoS One*, vol. 18, no. 1 January, 2023, doi: 10.1371/journal.pone.0278110. 740
741
742